

Duplicate Copy



FAIRCHILD
S P A C E

C10 #9480
CALL # 30-02

FSC-ESD-217-92-509

RTGs USING PbTe/TAGS THERMOELECTRIC ELEMENTS FOR MARS ENVIRONMENTAL SURVEY (MESUR) MISSION

Alfred Schock

July 1992

DISCLAIMER

This report was prepared as an account of work sponsored by an agency of the United States Government. Neither the United States Government nor any agency Thereof, nor any of their employees, makes any warranty, express or implied, or assumes any legal liability or responsibility for the accuracy, completeness, or usefulness of any information, apparatus, product, or process disclosed, or represents that its use would not infringe privately owned rights. Reference herein to any specific commercial product, process, or service by trade name, trademark, manufacturer, or otherwise does not necessarily constitute or imply its endorsement, recommendation, or favoring by the United States Government or any agency thereof. The views and opinions of authors expressed herein do not necessarily state or reflect those of the United States Government or any agency thereof.

DISCLAIMER

Portions of this document may be illegible in electronic image products. Images are produced from the best available original document.

RTGs USING PbTe/TAGS THERMOELECTRIC ELEMENTS FOR MARS ENVIRONMENTAL SURVEY (MESUR) MISSION

Alfred Schock

Fairchild Space and Defense Company
20301 Century Blvd.
Germantown, MD 20874
(301) 428-6272

Abstract

The paper describes the results of studies on an RTG option for powering the global network of unmanned landers for NASA's Mars Environmental Survey (MESUR) mission. RTGs are essentially unaffected by diurnal and seasonal variations, Martian sandstorms, and landing site latitudes, and their waste heat can stabilize the temperatures of the landers and their payload. The RTG designs described in this paper are based on PbTe/TAGS thermoelectric elements, in contrast to the SiGe-based RTGs the author described in previous publications. The RTGs described here differ not only in the choice of thermoelectric materials but also in the use of much lower operating temperatures, conductive rather than radiative heat transfer, an inert cover gas instead of vacuum in the RTG's converter, and fibrous instead of multifoil thermal insulation. As in a previous Teledyne design, the Fairchild designs described in this paper employ flight-proven General Purpose Heat Source modules and Close-Pack Arrays of thermoelectric converter modules. Illustrative point designs of RTGs producing 41 and 51 watts(e) at 28 volts are presented. The presented performance parameters were derived by detailed thermal, thermoelectric, and electrical analyses (including radiator geometry optimization) described in the paper. The Fairchild study resulted in modifications of the Teledyne design to permit scale-up to higher power levels, and to ensure adequate fuel clad ductility at launch temperatures and adequate thermal conductance from the thermoelectric cold ends to the RTG housing.

INTRODUCTION

NASA/JPL is studying a mission (MESUR) to distribute a large number (~16) of small unmanned landers over the surface of the Martian globe, ranging from equatorial to polar regions. When fully deployed, the robotic landers will form a global network to simultaneously collect seismic and meteorological data over a period of seven years. The scientific objectives of the mission will include data sampling relating to the internal structure of the Martian crust, global circulation, geochemistry of the soil, the chemical composition of residual polar caps, and high-resolution surface imaging. Particular emphasis will be placed on

hard-to-reach sites (polar deposits, rugged volcano flanks, etc.) that would be difficult or impossible to investigate by any other means. The sixteen landers are planned to be launched between 1999 and 2003. They may be preceded by a single lander (Pathfinder) launched in late 1996.

Since the scientific objectives require the simultaneous operation of the full network over an extended period of time, the sixteen landers (but not necessarily the Pathfinder) must be capable of long life. This requires either nuclear or solar power supplies (if the latter can operate during and after Martian sandstorms). Landers at high Martian latitudes ($>45^{\circ}$) require nuclear power systems (RTGs), which are independent of sun angle. The landers destined for low Martian latitudes could, if desired, employ solar power supplies, but that would require the development of two different landers for the high and low latitudes, and would necessitate the use of power-consuming electrical heaters to maintain the temperature of the solar-powered landers during the Martian nights.

To support the NASA/JPL mission studies, the Department of Energy's Office of Special Applications commissioned Fairchild Space and Defense Company to conduct related RTG design studies. Initially, the Fairchild studies had been focused on developing an RTG design that was rugged enough to survive high-g-level Martian impacts of a lander that had been decelerated by a parachute but without the use of retrorockets. Elimination of the retrorockets could greatly reduce the complexity and cost of the system. The Fairchild study succeeded in designing an RTG that - analysis indicated - would survive impacts up to about 2000 G [1]. Such hard-landing capability was shown to be adequate for survival of RTGs in suitably configured landers without retrorockets [1,2]. But such impact resistance would only permit hard landings if the rest of the lander's payload were similarly hardened. To avoid the necessity of doing that, JPL is presently leaning in the direction of limiting the lander's impact to 30 or 50 G, which is the peak G-level experienced during launch vibration and during entry into the Martian atmosphere. Eliminating the need for very high impact resistance expands the RTG design options available to the mission planner.

BACKGROUND

The MESUR RTG designs described in the author's previous papers [1,2] employed the same thermoelectric materials (SiGe) as those successfully used in recent flight programs (LES-8/9, Voyager, Galileo, Ulysses). They also employed the same General Purpose Heat Source (GPHS) modules [3] that were used in the Galileo and Ulysses RTGs [4] and will be used in the upcoming Cassini RTGs [5]. In addition, the MESUR RTG designs described in those papers employed thermoelectric multicouples similar to those used in the Modular RTGs [6] under development by DOE.

In addition to the above SiGe-based RTGs built by General Electric, another type of RTG employing PbTe and TAGS (Te-Ag-Ge-Sb) elements was developed and built by Teledyne Energy Systems and successfully flown on the Pioneer-10/11 and Viking missions. These RTGs differed from the GE units not only in the thermoelectric materials but also in operating temperatures (500°C versus 1000°C), heat source design (monolithic versus modular), heat transfer arrangement (conductive versus radiative), thermoelectric element configuration (spring-loaded versus cantilevered), RTG atmosphere (inert cover gas versus vacuum), and thermal insulation (fibrous versus multifoil). Such RTGs were used to power the two Viking Mars landers launched in 1975. They operated very reliably in the Martian atmosphere, and yielded about the same conversion efficiency as the SiGe RTGs despite their much lower hot-junction temperature.

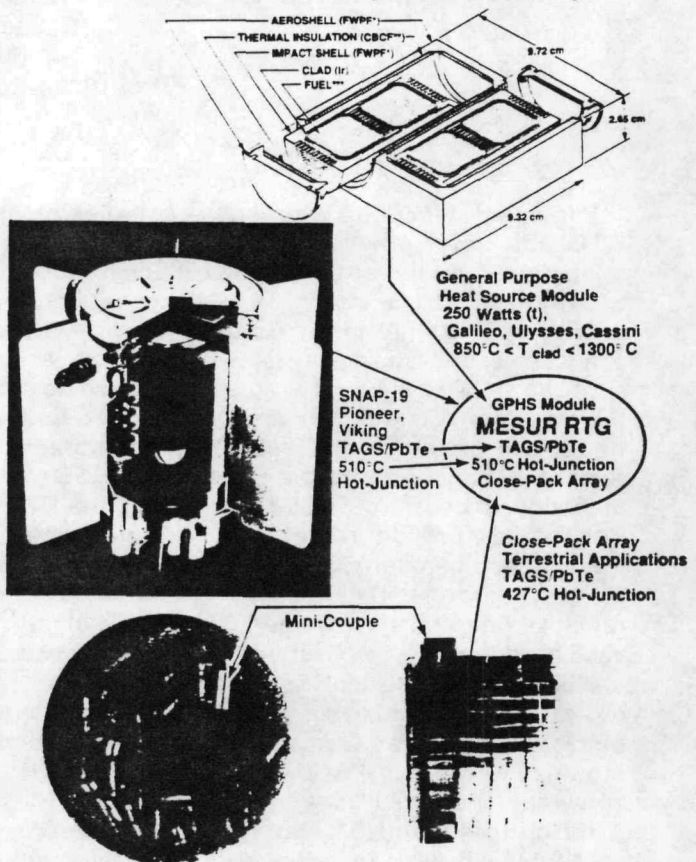
In spite of their proven development status and reliability, the Viking RTG design could not be used for the MESUR mission. In the first place, the facilities needed to produce the Viking heat source no longer exist; only the General Purpose Heat Source (GPHS) modules are presently available. In the second place, even if the Viking heat source could still be produced, it is not clear that it would meet today's more stringent safety requirements. And in the third place, an RTG based on the Viking design with individually spring-loaded thermoelectric elements would be too heavy and have too low an output voltage to meet the MESUR mission goals.

To overcome these shortcomings of the Viking design, Teledyne has proposed a conceptual design of a 15-watt RTG for the MESUR mission. The Teledyne design combines a GPHS module with high-voltage/low-mass Close-Pack Arrays of PbTe/TAGS thermoelectric elements. To balance the previous SiGe RTG studies, DOE has asked Fairchild to conduct an independent study of a MESUR RTG based on the same subsystems. This is the subject of the present paper.

TECHNOLOGY STATUS

The subsystems employed in the Teledyne design and their proposed operating temperatures are depicted in Figure 1, which summarizes their technology status.

Figure 1. Experience Base for Teledyne's MESUR RTG Design



The GPHS module has been subjected to very extensive safety analysis and safety tests to qualify it for launch on the Galileo and Ulysses missions. But it is only qualified if the operating temperature of the fuel capsule's iridium clad is above its ductile/brittle transition temperature (850°C).

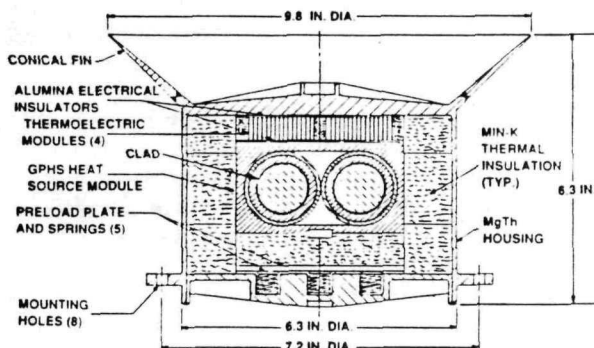
Close-Pack Arrays of thermoelectric elements have been successfully used by Teledyne in RTGs for a number of terrestrial applications, but not in space. Such arrays can substantially reduce the mass and increase the output voltage of the RTG. But Close-Pack Arrays have only been tested at hot-junction temperatures of 427°C, which is much below the postulated operating temperature of 510°C. On the other hand, the PbTe/TAGS materials have demonstrated their performance stability at the postulated 510°C hot-junction temperature in SNAP-19 RTGs for the Pioneer and Viking missions, but only in a configuration in which each thermoelectric leg is individually spring-loaded, not in compact arrays.

Thus, each of the proposed subsystems has been proven by itself, but not while operating together at the postulated temperatures. There is no obvious reason why they cannot be made to work together, but since it has not been done yet, some development and integration effort will be required.

MESUR RTG DESIGN

Figure 2 depicts Teledyne's proposed design of a 15-watt (BOM) RTG for the MESUR mission. As seen, it contains a single GPHS module sandwiched between spring-loaded Min-K insulation and the Close-Pack Thermoelectric Arrays. The spring load serves to support the heat source and the thermoelectric arrays, and to provide good thermal contact between the array's cold faces and the RTG housing (with its integral conical radiator.) The space between the sides of the square heat source module and the cylindrical RTG housing is filled with Min-K thermal insulation.

Figure 2. Teledyne 15-Watt RTG Design for MESUR
Using One GPHS Module and Close-Pack Thermoelectric Arrays



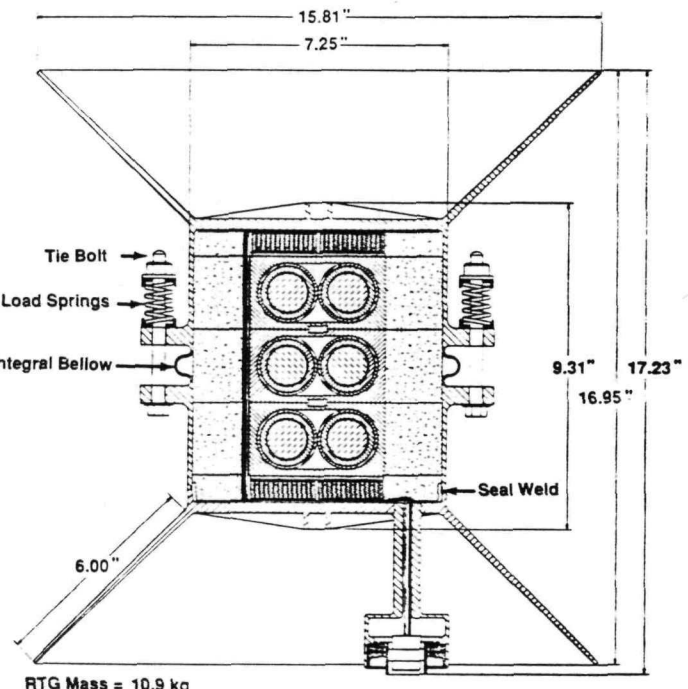
Fairchild's principal concerns about the design shown in Figure 2 related to its scalability to higher power levels, its excessively low iridium clad temperature (well below its ductile/brittle transition point), and doubts about the uniformity of the interface pressure between the thermoelectric cold ends and the housing. To address those concerns, Fairchild decided to design and analyze its own derivative of the Teledyne configuration.

FAIRCHILD DESIGN

The MESUR landers' design and power requirements have not been defined yet. Preliminary indications are that the MESUR Pathfinder power requirement may be in the range of 50 to 100 watts(e). The MESUR network landers are expected to require less power, because their later launch dates permit added time to develop more efficient payload components. Therefore, Fairchild decided to illustrate the scalability of its design derivative by roughly tripling the power output of the Teledyne design.

To achieve a significant increase above the Teledyne design's 15-watt level requires the use of more than one heat source module and the installation of Compact Thermoelectric Arrays on both ends of the heat source stack. This rules out Teledyne's method for applying the axial preload, since both ends of the heat source are occupied by thermoelectrics. Fairchild's proposed solution to this problem is to apply the axial preload on the outside of the RTG housing. This is illustrated in Figure 3, which shows an illustrative RTG design using three heat source modules.

Figure 3. Solution Proposed by Fairchild
3 Heat Source Modules, 41 Watts (e) BOM, 28.7 Volts

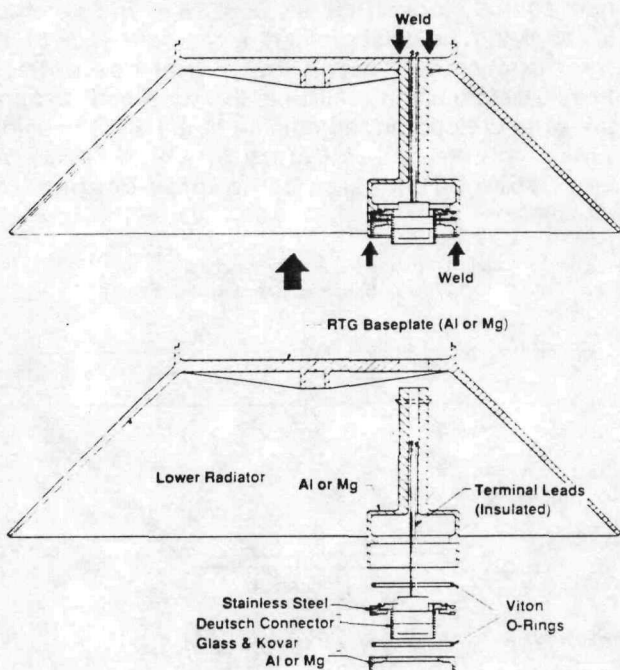


The key feature is to roll a flexible corrugation into a thin-walled section of the housing wall using a method similar to one employed in the fabrication of bellows. After the RTG housing is loaded and welded shut, four tie bolts and springs are applied to the housing's lugs to compress the flexible corrugation. This in turn applies a compressive load to the heat source stack and the thermoelectric arrays, as shown in Figure 3.

Figure 4 shows the feedthrough terminal through which the electrical power output emerges from the RTG. It employs a Deutsch connector with multiple pins glass-bonded to a Kovar sleeve. The Kovar is welded to a stainless steel flange, which is sealed to the magnesium housing extension by a pair of redundant Viton O-rings. This is identical to the arrangement that was successfully used in the Pioneer and Viking RTGs. It eliminates the need for a stainless-to-magnesium (or stainless-to-aluminum)

joint, and it provides a semi-permeable path for venting the helium generated by the radioisotope fuel's alpha decay to the Martian environment.

Figure 4. Baseplate and Terminal Connector



HELIUM VENTING

In SiGe RTGs for use in vacuum environments (e.g., Voyager, Galileo, Ulysses), the heat source is vented into the converter, which in turn is vented to the space vacuum after launch. This is feasible because the sublimation rate of SiGe (with a thin silicon nitride coating) is low enough to permit long-term operation at 1000°C without a cover gas. But in an external atmosphere as on Mars, simple venting of the SiGe converter to the outside would not be possible, because entry of the external atmosphere through the vent would quickly destroy the effectiveness of the multifoil thermal insulation. One way of coping with this problem is to insert a hermetic canister between the heat source and the converter [1, 7]. Thus, the heat source canister can be vented directly to the outside, without affecting the vacuum in the converter. But the addition of a reliable high-temperature canister would require additional development and would significantly increase the RTG mass.

In the case of PbTe/TAGS RTGs, the converter must contain an inert cover gas to prevent excessive sublimation of the thermoelectric materials. Fortunately, the operating temperatures in these RTGs are low enough to permit the use of fibrous (Min-K) thermal insulation. Unlike multifoil, Min-K remains a fairly effective thermal insulator even in the presence of high helium pressure. Thus, there is no need for a canister, since the heat source's helium can be vented into the converter.

To prevent the long-term buildup of excessively high helium pressure in the RTGs, it must be slowly vented to the outside. This was done in the Viking RTGs by means of semi-permeable Viton O-rings, and was also adopted in Teledyne's MESUR RTG design and in Fairchild's derivative design. The Viton O-rings will necessarily permit some inleakage of the Martian atmosphere into the RTG. But the inleakage rate will be much slower than the helium outleakage because the external pressure on Mars is much lower than the RTG's internal pressure, and because the permeability of Martian gases (mostly CO_2) through Viton is much lower than that of helium. Experience on the Viking mission has shown that inleakage of Martian gases had no significant effect on RTG performance, as long as the small amount of oxygen that gets in is gittered by zirconium.

FUEL CLAD DUCTILITY

The Teledyne design shown in Figure 2 depicts the hot ends of the thermoelectric arrays pressing directly against the heat source, without intervening thermal insulation. That would lead to an unacceptably low iridium clad temperature, since the thermoelectric hot-junction temperature is only 510°C (compared to 1000°C in the Galileo and Ulysses RTGs). The clad temperature must be raised above 850°C to achieve sufficient iridium ductility for surviving launch pad impacts without fuel release. This requires the addition of a thermal insulation layer between the thermoelectric hot face and the adjacent heat source face. Fairchild initially investigated the use of pyrolytic graphite, but this was found unattractive since a thickness of more than 2 cm would be required to achieve the desired clad temperature. Subsequently, it was found that Min-K is so much more effective as a thermal insulator, even in the presence of a helium atmosphere, that a thickness of less than a mm would suffice to raise the clad temperature above its ductile-to-brittle transition point. Such a layer of Min-K is reflected in the design depicted in Figure 3 and in subsequent figures.

ALTERNATIVE FUEL CLAD OPTION

An alternative solution to the clad ductility problem would be to substitute a platinum/rhodium alloy for the iridium alloy used in SiGe RTGs. That alloy (Pt-3008) has been successfully used for the 1-watt Radioisotope Heater Units (RHUs), many of which were flown on the Galileo mission and will be flown on the Cassini mission. Both the platinum alloy and the iridium alloy form eutectics with carbon, but the eutectic melting point is much lower for the platinum alloy than for iridium (1760°C versus 2200°C). Pt-3008 was not deemed suitable for use in evacuated SiGe RTGs with their 1000°C hot-junction temperature and 1300°C clad temperature; but it could be quite suitable for use in the helium-filled PbTe/TAGS RTGs with their 510°C hot-junction temperature.

The chief advantage of the platinum alloy over iridium would be its room-temperature ductility. Thus, there would be no need for a thermal insulation layer between the thermoelectric hot junctions and the heat source. This would significantly lower the heat source's temperature and the heat loss through the insulation between its sides and the housing, resulting in increased RTG efficiency and power.

Additional advantages of the platinum over iridium alloy are its lower cost, much easier fabricability and weldability, and better oxidation resistance. However, considerable development effort and safety testing would be required to qualify it for use in PbTe/TAGS flight RTGs. For those reasons, it was not used in the present baseline design, in spite of its potential advantages.

AXIAL PRELOAD

Finally, one other design aspect requiring discussion is the interface pressure between the thermoelectric cold faces and the RTG end caps. Teledyne had advised that an interface pressure of 200 psi was needed to produce adequate thermal conductance at that interface, and this was initially adopted as a design goal in the Fairchild study. 200 lbs per square inch of thermoelectric face area corresponds to a total axial preload force of 2900 lbs for the RTG. Such a force could be easily produced by the external load springs shown in Figure 3. However, ensuring the uniformity of the interface pressure across the thermoelectric cold face proved much more difficult than had been anticipated. The interface pressure would be quite uniform if the heat source modules and the RTG end caps were infinitely stiff. But they are not. Each end cap is loaded at its rim by the spring-loaded housing, and that load is balanced by the much smaller area of the thermoelectric arrays at the center of the end cap. Under those conditions, the end caps will bow, with the interface pressure concentrated near the boundary of the square converter array, and no pressure (in fact, a gap) at its center. Detailed structural analyses were performed by Fairchild to assess the effectiveness of thickening the end cap wall and adding stiffening ribs. But these measures had only limited success. They substantially increased the mass of the RTG, but still left a significantly lower interface pressure near the array's center than near its outside.

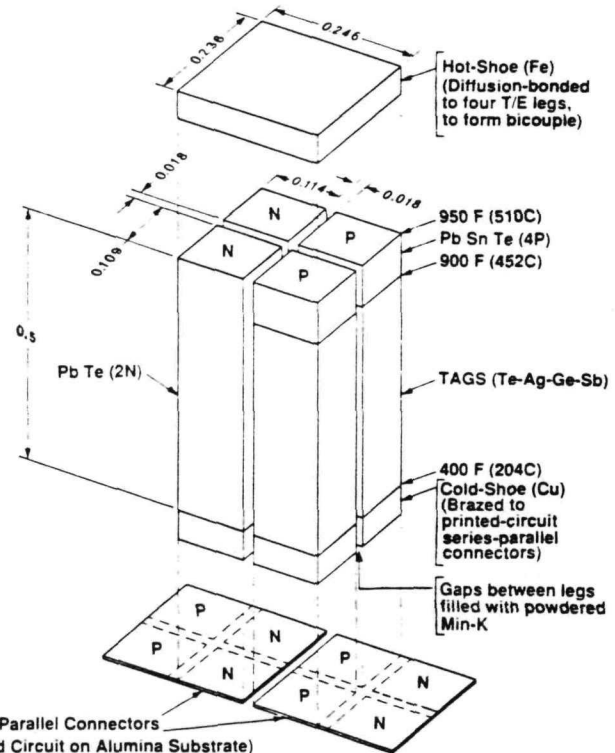
At this point, Fairchild recognized that there really is no need for the 200 psi minimum interface pressure that had been specified by Teledyne. Such a high pressure would indeed be required in a vacuum RTG to lower the contact resistance, but not in a helium-filled RTG. Simple thermal analysis revealed that at the projected heat flux leaving the array's cold face, a gap due to bowing of the end cap would only produce a temperature drop of 6°C per mil of gap width. Thus,

a peak gap of 1 or 2 mils would be quite acceptable. Such small gaps can be achieved, especially since the high axial preload (2900 lbs) for thermal conductance is no longer needed. The only preload requirement left is that needed to support the stack of heat source modules during launch and during entry into the Martian atmosphere. To determine that, detailed structural analyses are currently under way.

THERMOELECTRIC CONVERTER DESIGN

Figure 5 shows the design dimensions and materials of the thermoelectric elements. As in the Viking RTGs, they employ PbTe(2N) n-legs and TAGS p-legs. Since TAGS has a more limited high-temperature capability than PbTe, it is followed by a PbSnTe(4P) segment at the p-leg's hot end. The legs were dimensioned to duplicate Teledyne's temperature difference between their hot- and cold-junctions for the computed heat flow rates.

Figure 5. Thermoelectric Bicouple



Each leg contains a copper cold-shoe at its cold end. The legs are arranged in groups of four (two n and two p), whose hot ends are diffusion-bonded to an iron hot shoe to form a bicouple. Alternatively, it would be possible to cut the hot shoe in half, so that each one forms a series connection between a unicouple's n- and p-legs. But that would double the number of elements, and the unicouples would be less stable against lateral g-loads than the bicouples. As in the Teledyne design, the gaps between adjacent legs are filled with powdered Min-K thermal insulation.

The cold ends of the thermoelectric modules' bicouples are brazed to series-parallel connectors in the form of a printed circuit on an alumina (or alternatively Kevlar) substrate. Thus, the thermoelectric circuit consists of double strings of couples, with parallel cross-connections at their hot and cold ends. The parallel cross-connections permit continued operation of the series string in spite of open-circuit failures of individual couples.

The thermoelectric circuit and its current path are depicted in Figures 6 and 7 for the converters at the bottom and top of the heat source, respectively. As seen, each end of the heat source stack is covered with four thermoelectric modules, and each module contains $14 \times 14 = 196$ legs forming 49 bicouples. The arrows show the electrical current directions. As shown, each module produces 3.5 volts. The eight modules (top and bottom) are connected in series, yielding a total RTG output of 28 volts to match the expected load demand. This eliminates or minimizes the need for power-consuming DC-to-DC converters. As shown, both RTG terminals are next to each other at the bottom of the generator, to facilitate connections to the vacuum feedthroughs at the RTG baseplate. A series of figures depicting the detailed assembly and fueling sequence culminating in the RTG depicted in Figure 3 was prepared, but was deemed too long to include in the present paper.

Figure 6. Current Path Through Lower Thermoelectric Modules (4)

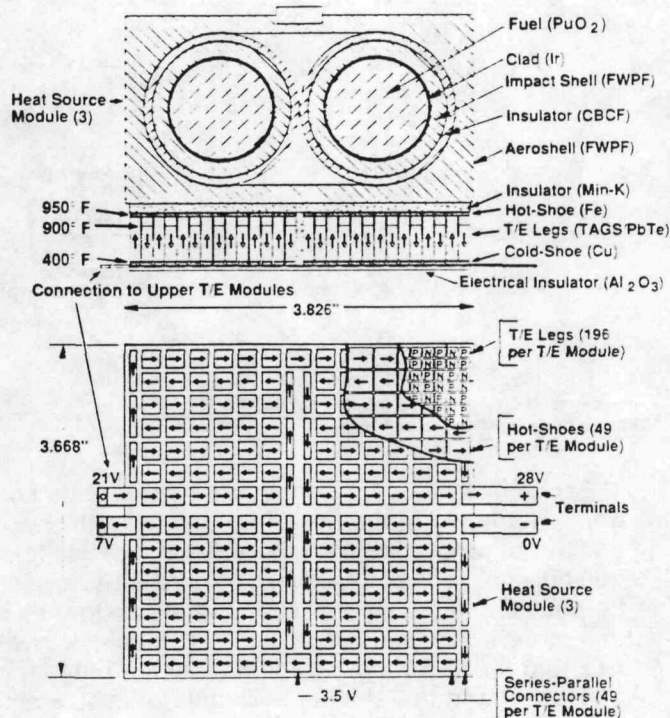
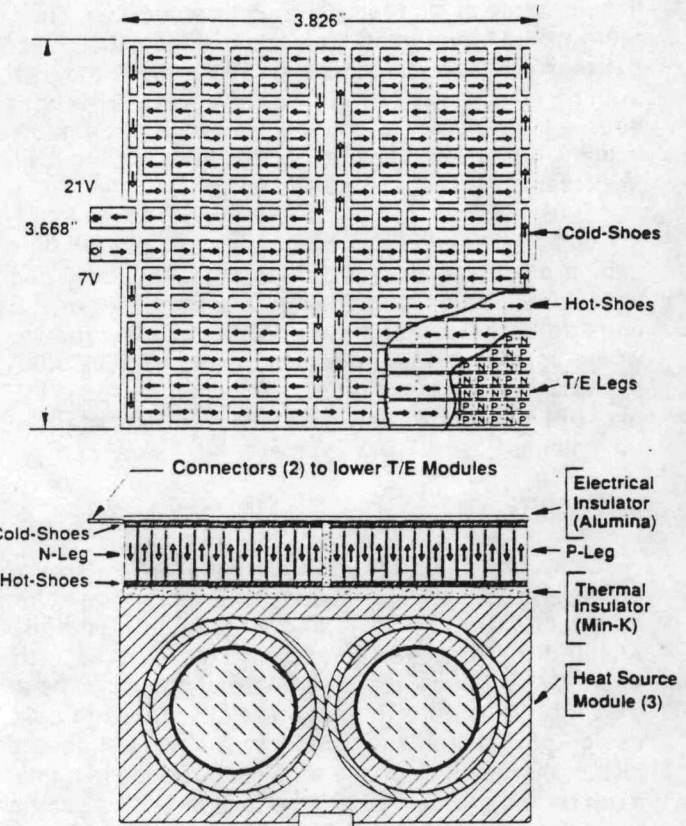


Figure 7. Current Path Through Upper Thermoelectric Modules (4)



THERMAL AND ELECTRICAL ANALYSES

The analyses were based on Teledyne-supplied data on the temperature-dependent Seebeck coefficient S , electrical resistivity ρ , and thermal conductivity k of the thermoelectric n- and p-legs shown in Table 1.

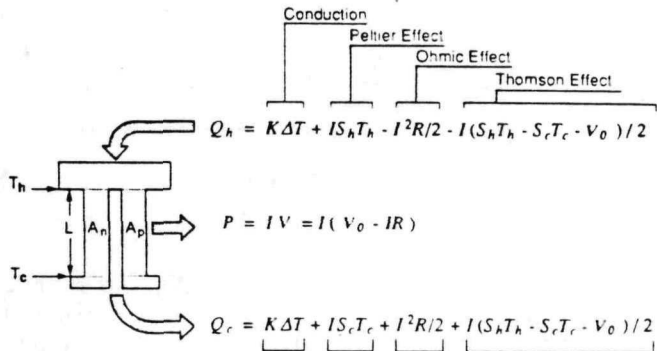
Table 1. Temperature-Dependent Thermoelectric Properties

Temp. °C	Seebeck Coefficient Microvolt °C			Electrical Resistivity mΩ · cm			Thermal Conductivity Watt · m °C		
	PbTe	TAGS	PbSnTe	PbTe	TAGS	PbSnTe	PbTe	TAGS	PbSnTe
593	-213	195	193	4.67	1.59	3.10	1.40	1.98	2.32
566	-226	201	190	4.62	1.58	3.02	1.37	1.93	2.13
538	-236	202	186	4.55	1.57	2.88	1.33	1.87	2.01
510	-242	204	180	4.45	1.56	2.70	1.31	1.80	1.95
482	-246	206	172	4.31	1.55	2.49	1.30	1.74	1.93
454	-248	206	163	4.10	1.53	2.29	1.30	1.68	1.95
427	-247	206	152	3.84	1.51	2.09	1.31	1.64	2.00
399	-244	203	141	3.53	1.49	1.91	1.35	1.61	2.05
371	-239	199	130	3.21	1.46	1.75	1.38	1.60	2.13
343	-232	195	118	2.88	1.43	1.61	1.45	1.58	2.20
316	-224	189	105	2.55	1.39	1.48	1.52	1.57	2.27
288	-215	183	93	2.22	1.34	1.38	1.61	1.57	2.34
260	-205	176	81	1.92	1.29	1.28	1.71	1.56	2.40
232	-195	168	70	1.63	1.24	1.19	1.82	1.55	2.46
204	-184	159	59	1.37	1.19	1.12	1.94	1.55	2.54
177	-173	150	49	1.14	1.15	1.04	2.04	1.54	2.51
149	-162	139	40	0.94	1.10	0.97	2.19	1.53	2.70
93	-141	115	26	0.60	1.05	0.84	2.46	1.52	3.08
38	-119	90	17	0.34	0.89	0.72	2.77	1.50	3.40
10	-110	77	13	0.23	0.84	0.64	2.94	1.50	3.63

For given hot- and cold-junction temperatures, these data were used to compute temperature-averaged values of the three parameters for each leg.

A detailed 3-dimensional thermal model of the RTG design was constructed. It assumed that all heat rejection is radiative, with the MESUR lander which surrounds the RTG acting as a heat sink at 100°F (38°C). The thermal model accounted for radiative interchanges between all points of the RTG housing and radiators within view of each other. Heat flow through the thermoelectric elements took account of conduction, Peltier cooling, Ohmic heating, and Thompson effects. (See Figure 8). Since three of these four items are current-dependent, the thermal and electrical analyses had to be carried out in a coupled manner [8]. The portion of the heat flow converted to electricity was modeled as an effective heat sink.

Figure 8. Unicouple Energy Balance



The RTG performance analysis had to be carried out iteratively, since the thermal conductivity of the Min-K depends on its temperature (Figure 9) and on the helium pressure (Figure 10), which is a function of the

Figure 9. Effect of Temperature T on Thermal Conductivity k of Min-K-1800

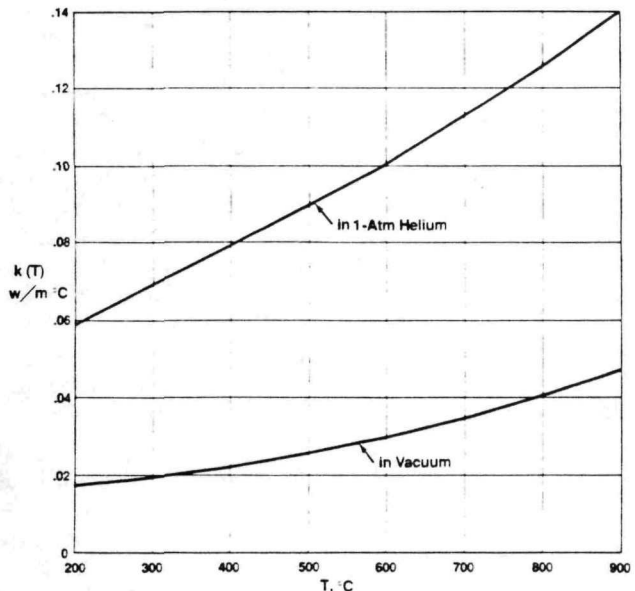
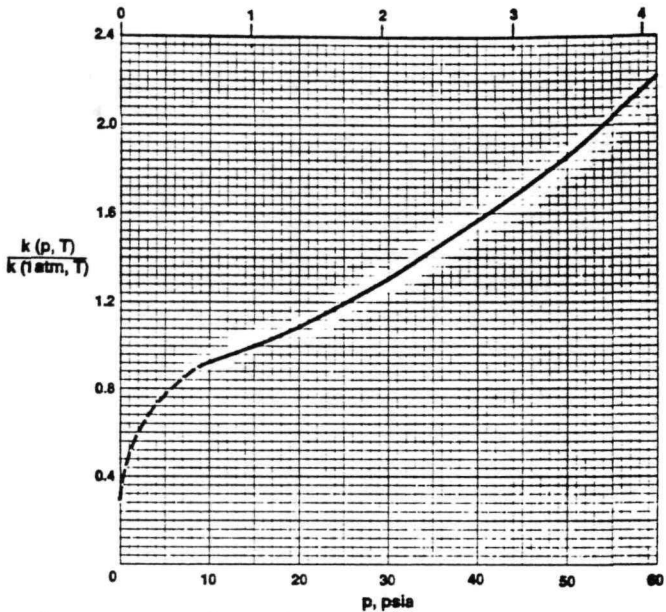
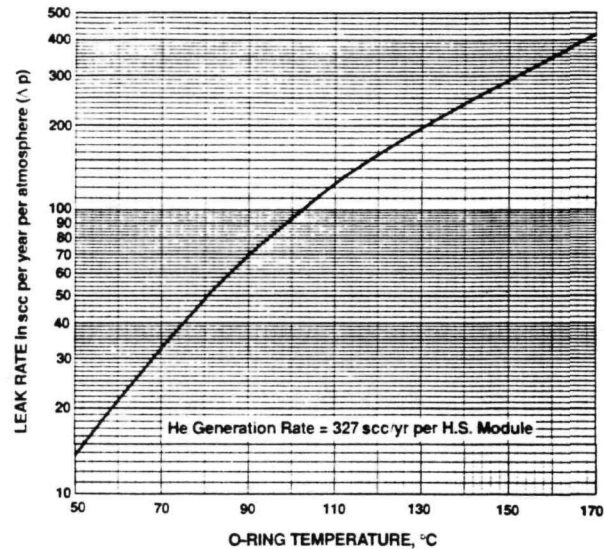


Figure 10. Effect of Helium Pressure p on Thermal Conductivity k of Min-K-1800
p, atmospheres



temperature-dependent permeability of the Viton O-rings (Figure 11). The data in these figures were derived from Teledyne measurements performed during the Pioneer and Viking programs.

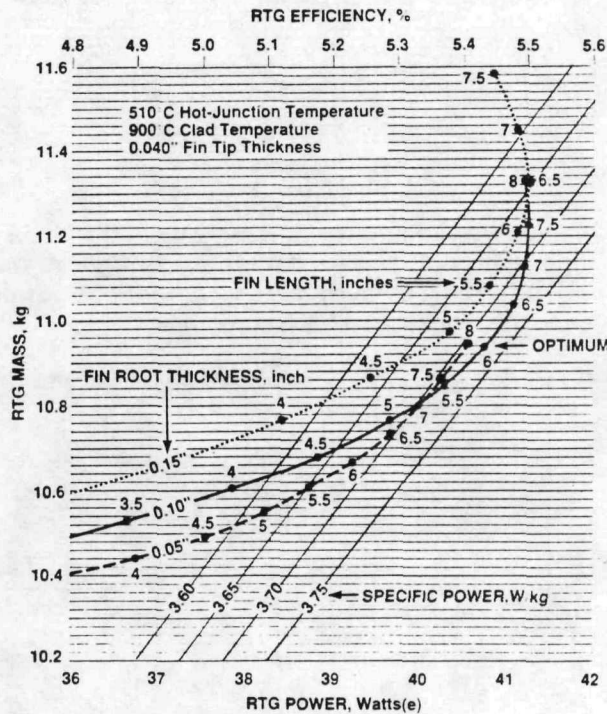
Figure 11. Effect of Temperature on Helium Leak Rate Through VITON Seals (Two O-Rings in Series)



The Fairchild analyses assumed that the helium pressure was at equilibrium, with the outleakage equal to the helium generation rate due to alpha decay (327 scc per year per heat source module). For any given radiator design, the thermoelectric leg length was iteratively adjusted until the resultant hot-junction temperature matched the corresponding Teledyne value of 510°C, and the insulator thickness between the T/E hot shoes and the heat source was adjusted to yield a clad temperature of 900°C.

The radiator design was then optimized by varying the conical fin length and fin root thickness to find the combination that maximizes the RTG's specific power. This is illustrated in Figure 12, which shows the effect of the radiator's fin geometry on the RTG's power and mass. Each of the displayed points represents a specific RTG design with a hot-junction temperature of 510°C and a clad temperature of 900°C. As shown, increasing fin lengths lead to lower cold-junction temperatures and consequently to higher output powers and efficiencies. Of course, they also lead to higher RTG weights.

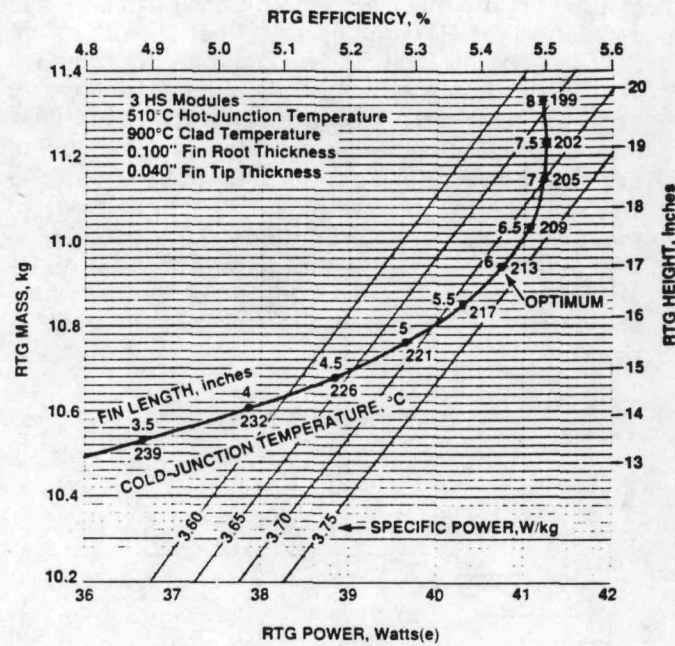
Figure 12. Effect of Radiator Fin Geometry on Specific Power of 3-Module RTG



The four diagonals represent lines of constant specific power. As can be seen, specific power for this design is maximized at a fin root thickness of 0.100" and a fin length of 6 inches, for a peak value of 3.73 watts(e) per kg. For thinner or shorter fins, the specific power goes down because of higher cold-junction temperatures, resulting in lower efficiency and power. For thicker or longer fins, the specific power decreases because of higher radiator mass.

For the optimum fin root thickness of 0.100", Figure 13 displays the effect of the radiator's fin length on the thermoelectric cold-junction temperature and on the RTG's power, mass, efficiency, length, and specific power. As can be seen, the specific power maximizes at a cold-junction temperature of 213°C (415°F), which is close to the 400°F value assumed in the Teledyne design.

Figure 13. Effect of Radiator Fin Length on Cold-Junction Temperature and on Power, Mass, Length, Efficiency, and Specific Power



The figure is also useful for assessing the effect of design trade-offs, by departing from the maximum-specific-power point. For example, reducing the fin length from 6" to 4" would reduce the RTG's length from 17" to 14" and its mass from 10.94 to 10.59 kg, but at the cost of reducing its power by 7% (from 40.8 to 37.9 watts(e)), with corresponding decreases in efficiency and specific power. Such trade-offs may be desirable if the space for the RTG in the lander is severely constrained.

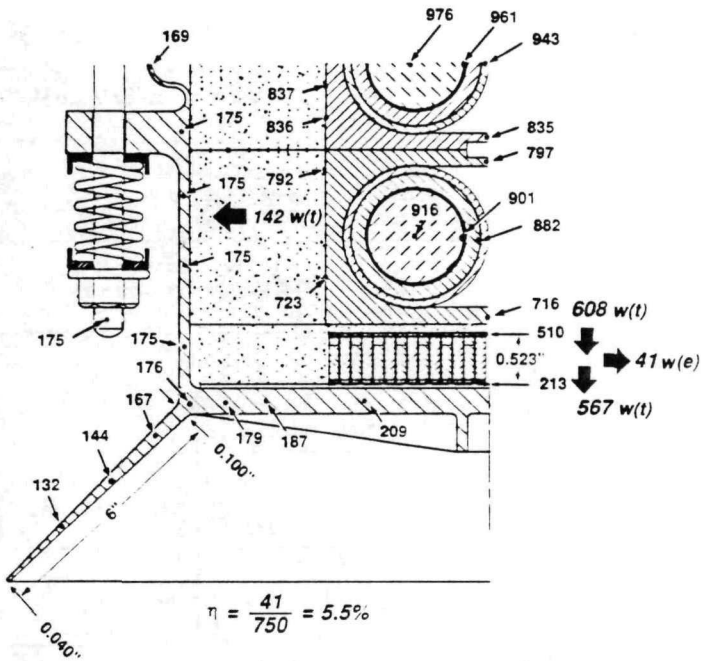
OPTIMUM-DESIGN PERFORMANCE

The salient temperatures and energy balance for the maximum-specific-power design identified in Figures 12 and 13 are depicted in Figure 14. These are for a Min-K thickness of 0.030" and a thermoelectric leg length of 0.523", to meet the hot-junction and clad temperature goals. Note that the clad temperatures are well above iridium's ductile-to-brittle transition point (850°C) and far below the point at which excessive grain growth would occur (1300°C). In addition, the RTG housing temperatures are seen to be much lower than the corresponding 250°C temperature of the SiGe RTGs used on the Galileo and Ulysses missions. This should avoid any creep-induced load relaxation effects.

The figure also shows the fin length (6"), fin root thickness (0.10"), and fin tip thickness (0.04") of the conical radiators, and summarizes the RTG's energy balance. Out of the 750 thermal watts generated by the three heat source modules at beginning of life, 142

watts(t) are lost through the Min-K side insulation and 608 watts(t) are delivered to the hot sides of the thermoelectric modules. Of those, 41 watts are converted to electrical power and 567 watts(t) are rejected to the RTG housing for radiation to the surrounding spacecraft. This rejected heat enables the spacecraft's payload temperature to be relatively independent of variations in solar input. The total mass of the RTG (with a magnesium-alloy housing, as in the Viking and Pioneer RTGs) is 10.9 kg, yielding a specific power of 3.73 watts(e)/kg. The RTG has a thermoelectric efficiency of $41/680=6.7\%$ and a system efficiency of $41/750 = 5.5\%$.

Figure 14. RTG Temperature Distribution (C) and Energy Balance of 3-Module RTG



FOUR-MODULE RTG

Next, it was decided to investigate whether the same design approach could be applied to an RTG with four heat source modules, to increase its power output. Analyses to optimize the radiator fins for a 4-module RTG yielded the results displayed in Figure 15, which is analogous to Figure 12 for the 3-module RTG. As shown, the specific power is maximized (at 3.70 watts/kg) by 8"-long fins with a 0.150" root thickness. The larger fins are needed because of the higher heat rejection rate of the 4-module RTG. Because of the higher heat flux through the thermoelectric legs, their length was reduced from 0.523" to 0.363" to maintain the same 510°C hot-junction temperature.

The optimum 4-module design identified in Figure 15 is displayed in Figure 16, which is analogous to the 3-module design in Figure 3.

Figure 15. Effect of Radiator Fin Geometry on Specific Power of 4-Module RTG

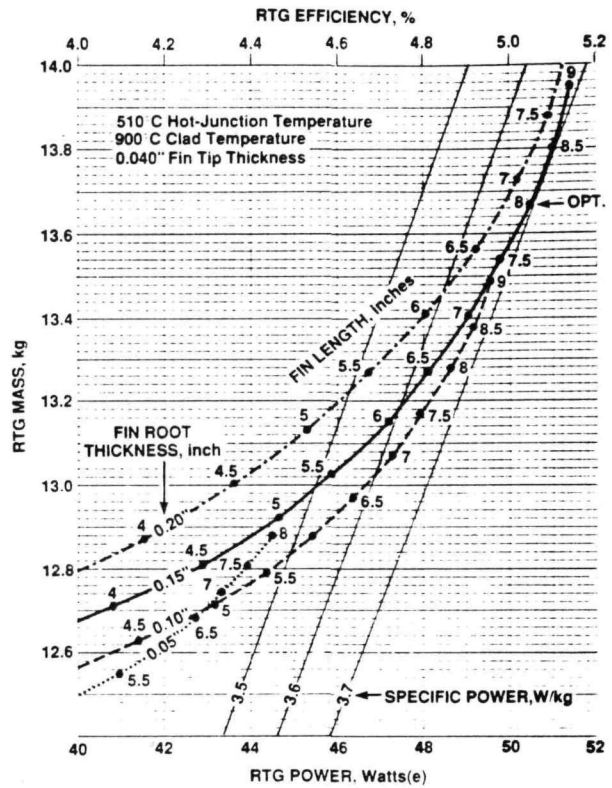


Figure 16. Alternative Design Option
4 Heat Source Modules, 51 Watts(e) BOM, 28.7 Volts

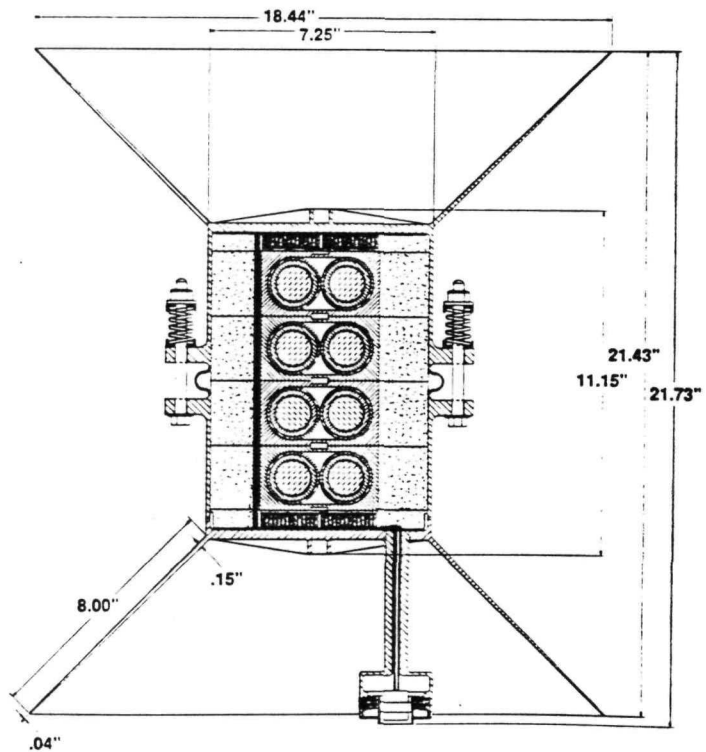
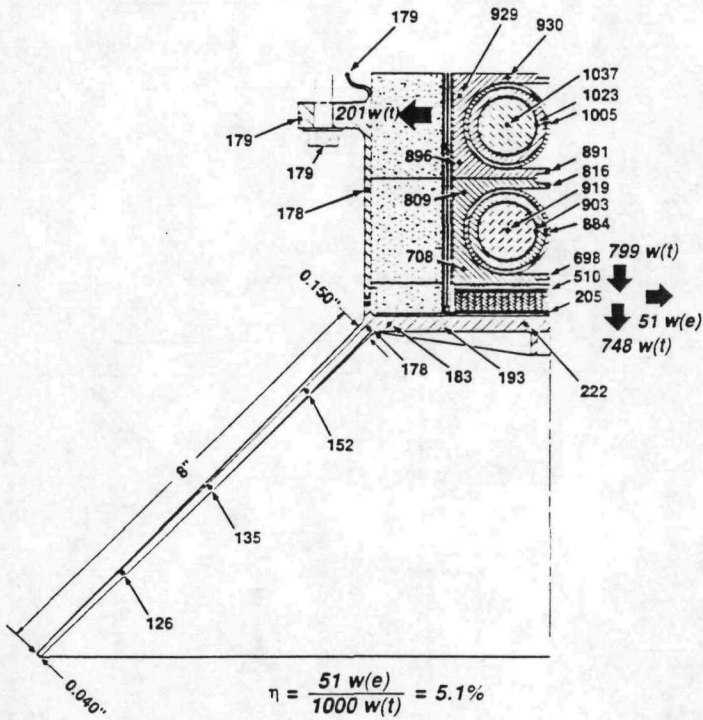


Figure 17 shows the key temperatures and energy balance of the four-module design. As seen, the operating temperatures of the inner and outer fuel clads are 1023° and 903°C. These are still well within the acceptable operating range of 850°C to 1300°C for the iridium. Comparison of the analogous Figures 17 and 14 shows that the sides of the four-module heat source are substantially hotter than those of the three-module heat source. As a result of the higher temperature and greater length, the heat loss through the Min-K insulation is significantly higher (201 versus 142 watts) and the RTG's system efficiency is substantially lower (5.1 versus 5.5%). Thus, increasing the number of heat source modules yields diminishing returns in increased RTG power (51 watts for the 4-module RTG versus 41 watts for the 3-module case). Also, the four-module design optimizes at a much larger and heavier radiator. The resultant RTG mass (with a magnesium housing) is 13.7 kg. But because of the higher power output (51 versus 41 watts), the specific powers of the two RTGs are quite close (3.70 versus 3.73 w/kg).

Figure 17. RTG Temperature Distribution (C) and Energy Balance of 4-Module RTG



The design parameters and mass breakdowns of the two Fairchild designs (Figures 3 and 16) and of the earlier Teledyne design (Figure 2) are summarized in Tables 2 and 3, respectively. (It should be noted that the listed performance parameters for the Teledyne design were computed by them, and were not based on independent Fairchild analyses.) As can be seen, Fairchild's thermoelectric leg dimensions and gaps are quite similar to those proposed by Teledyne. Thus, they should not result in any added development problems.

Table 2. RTG Mass Summary (with Mg Housing)

RTG Design	Teledyne	Fairchild	
Number of Heat Source Modules	1	3	4
RTG Power, Watts (e)	15	41	51
Mass Breakdown, kg:			
Heat Source Modules	1.43	4.30	5.74
Housing Fin Assembly	1.20	2.62	3.83
Min-K Thermal Insulation	0.36	1.13	1.39
Thermoelectric Modules	0.65	1.95	1.65
Alumina Insulators	0.06	0.25	0.25
Preload Elements	0.12	0.48	0.57
Receptacles, O-Rings, etc.	0.09	0.21	0.23
TOTAL	3.92	10.94	13.66

Table 3. MESUR RTG Design Comparison

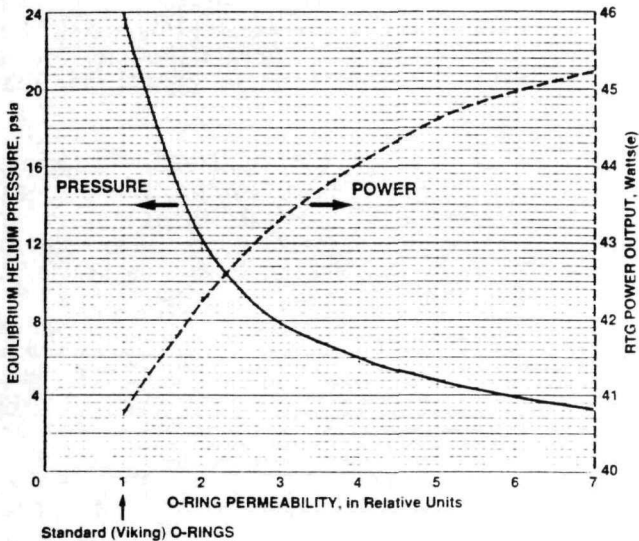
Teledyne		Fairchild		
1 250 W(t)	3 750 W(t)	4 1000 W(t)	Stacked Heat Source Modules Thermal Power	
15 W(e) 12 V 6.0%	41 W(e) 28.7 V 5.4%	51 W(e) 28.7 V 5.1%	Power Output (BOM) Voltage Output RTG Efficiency	
1 4 164	2 4 196	2 4 196	Active Heat Source Faces T/E Modules per Active HS Face T/E Legs per Module	
0.500" 0.102" 0.102" 0.014"	0.523" 0.114" 0.109" 0.018"	0.363" 0.114" 0.109" 0.018"	Leg Length Leg Width Leg Thickness Interleg Gap	
328 2 164	784 2 392	784 2 392	Couples per RTG Parallel Couples per Bicouple Bicouples in Series	
3" — —	6" 0.10" 0.04"	8" 0.15" 0.04"	Conical Fin Length Fin Root Thickness Fin Tip Thickness	
3.9 kg 3.85	10.9kg 3.73	13.7 kg 3.70	RTG Mass (Mg Housing) Specific Power (Mg), w/kg	

ALTERNATIVE DESIGN OPTIONS

Finally, we wish to examine the effect of two alternative design options on the performance of an RTG with three heat source modules. Both options are based on the observation that the heat loss through the Min-K side insulation is substantial, as shown in Figures 14 and 17. If that loss could be significantly reduced, it would raise the RTG's power and efficiency.

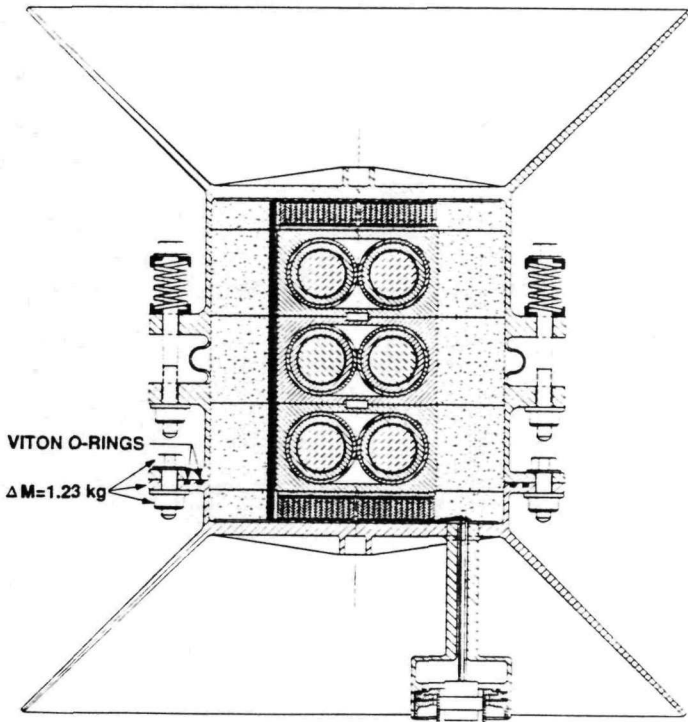
One way of reducing the heat loss through the Min-K insulation would be to reduce the RTG's equilibrium helium pressure, by increasing the leak rate through the Viton O-rings. This is illustrated in Figure 18, which shows the effect of O-ring permeability on helium pressure and RTG power. As can be seen, significant power improvement is possible.

Figure 18. Effect of VITON O-Ring Permeability on Helium Pressure and RTG Power



The O-ring's leak rate can be increased by raising their temperature or their size. Higher temperatures are risky, because they would exceed the existing experience base. Larger O-rings are practical, as illustrated in the Option A design shown in Figure 19. Here the housing seal weld of the Figure 3 baseline design has been replaced by redundant large-diameter O-ring seals. As seen, this required the addition of bolted flanges, which increased the RTG mass by 1.23 kg.

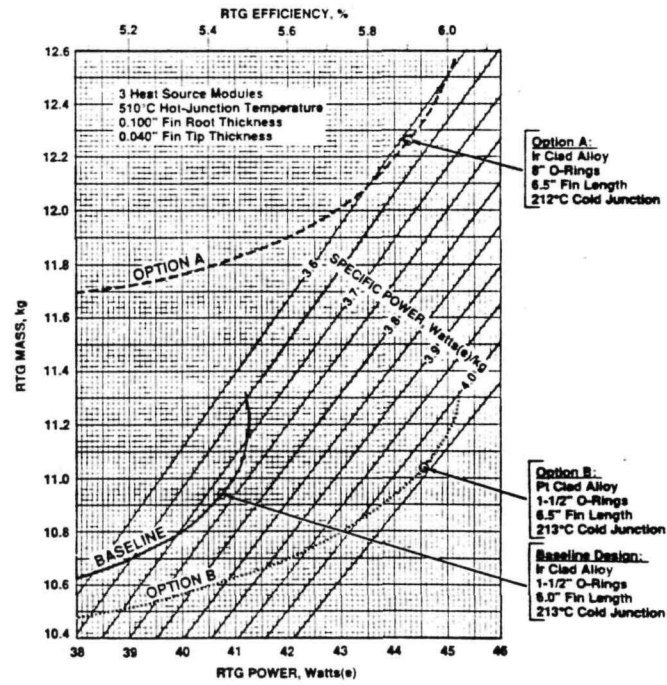
Figure 19. RTG Sealed with VITON O-Rings (Option A)
To Quadruple Helium Leak Rate, Reduce Equilibrium Pressure and Min-K
Conductivity, to Raise Output Power and Efficiency



The other design alternative, Option B, is virtually identical to the baseline design (Figure 3), except that the iridium-alloy fuel clads have been replaced by the platinum-alloy (Pt-3008) used in Radioisotope Heater Units (RHUs). Since loss of ductility at low operating temperatures is not a concern with this alloy, this substitution permits the elimination of the Min-K insulation between the thermoelectric hot faces and the heat source's end faces. As a result, the heat source operating temperature is reduced, the heat loss through the side insulation is diminished, and the RTG's power and efficiency are increased.

The two design alternatives were analyzed as before, and Figure 21 compares their performance parameters (power, mass, efficiency, and specific power) to those of the baseline design. The three curves in that figure are all for the case of three heat source modules and the Teledyne-recommended hot-junction temperature of 510°C (900°F). All are for the optimum fin root thickness (0.100") and the same fin tip thickness (0.040"). For each curve, the implicit variable is the fin length, and the circled point indicates the fin length that maximizes the specific power. The corresponding call-outs list the optimum fin length and cold-junction temperatures for the three designs. As seen, these parameters are almost the same for the three cases.

Figure 20. Comparative Performance of Alternative Design Options



Comparison of the two options with the baseline design show that they both yielded significant increases (-9%) in power and efficiency. But in the case of Option A (the O-ring-sealed RTG) the increased power is outweighed by the added mass of the seal flanges and bolts, so that its specific power is

actually lower (-9%) than that of the baseline design. Therefore, the desirability of Option A comes down to the relative importance of power (or efficiency) versus specific power.

In the case of Option B (with Pt-3008 clads), the power gain is achieved without any significant mass penalty, so that the RTG's specific power would be increased from 3.73 to 4.04 watts/kg. Whether the resultant gain in power, efficiency, and specific power would justify the required development effort and safety tests is up to DOE management.

CONCLUSIONS

In general, the Fairchild RTG study described in this paper showed that, with appropriate modifications, the Teledyne design based on use of the flight-proven GPHS heat source modules and on Close-Pack PbTe/TAGS thermoelectric arrays can be scaled up to higher power levels (within limits); and that solutions to ensure adequate iridium ductility at launch temperature and to provide adequate thermal conductance from the thermoelectric cold face to the RTG housing are available.

Acknowledgments

The author wishes to express his appreciation of the cooperative attitude of Mr. Wayne Brittain of Teledyne Energy Systems and the support of Dr. Emil Skrabek in furnishing the data needed for carrying out the Fairchild study. He also wishes to acknowledge the contributions of Dr. Heros Noravian of Analytix in implementing the thermal and electrical analyses and of Mr. Kumar Sankarankandath in preparing the design illustrations, and appreciates the support of the Department of Energy's Office of Special Applications, R. Lange (Director) and E. Mastal (Deputy).

References

- [1] Schock, A. (1991) "Design of Small Impact-Resistant RTGs for Global Network of Unmanned Mars Landers," 42nd Congress of the International Astronautical Federation, held in Montreal, Canada.
- [2] Schock, A. and M. Mukunda (1992) "RTG Impact Response to Hard Landing During Mars Environmental Survey (MESUR) Mission," for presentation at the 27th Intersociety Energy Conversion Engineering Conference, held in San Diego, CA.
- [3] Schock, A. (1980) "Design Evolution and Verification of the General Purpose Heat Source," #809203 Proc. of the 15th Intersociety Energy Conversion Engineering Conference, held in Seattle, WA.
- [4] Schock, A. and H. Sookiazian (1979) "Design, Analysis, and Optimization of RTG for Solar Polar Mission," Proc. of the 14th Intersociety Energy Conversion Engineering Conference, held in Boston, MA.
- [5] Schock, A., H. Noravian, C. Or, and K. Sankarankandath (1991) "Design and Analysis of RTGs for CRAF and Cassini Mission," Trans. of the 8th Symposium on Space Nuclear Power Systems, held in Albuquerque, NM.
- [6a] Schock, A. (1981) "Modular Isotopic Thermoelectric Generator," #819174 Proc. of the 16th Intersociety Energy Conversion Engineering Conference, held in Atlanta, GA.
- [6b] Schock, A. (1983) "Revised MITG Design, Fabrication Procedure, and Performance Predictions," Proc. of the 18th Intersociety Energy Conversion Engineering Conference, held in Orlando, FL.
- [7a] Schock, A., K. Sankarankandath, and M. Shirbacheh (JPL) (1989) "Requirements and Designs for Mars Rover RTGs," Proc. of the 24th Intersociety Energy Conversion Engineering Conference, held in Washington, D.C.
- [7b] Schock, A. (1989) "Mars Rover RTG Study," 40th Congress of the International Astronautical Federation, held in Malaga-Spain.
- [8] Schock, A., H. Noravian, and C. Or (1990) "Coupled Thermal and Electrical Analysis of Obstructed RTGs," Proc. of the 25th Intersociety Energy Conversion Engineering Conference, held in Reno, NV.